Paper

Pyroelectric Infrared Sensor Using Modified $PbTiO_3$ Ceramics

Masayuki Nakamoto* Member　Nobuo Iwase*** Non-member
Noboru Ichinose** Member　Youhachi Yamashita* Non-member

Pyroelectric infrared sensor using $(Pb_{1-x}, Ca_x)[(Co_{1/2}W_{1/2})Ti]O_3$ ceramics have been studied by changing Ca concentration, the infrared ray absorbing film diameter, and the electromagnetic wave shielding materials for packaging. With an increase in Ca concentration from x=0.05 to 0.28, the pyroelectric coefficient P and the figure of merit Fv increased and reached 4.43×10^{-8} $Ccm^{-2}℃^{-1}$, and 0.61×10^{-10} $CcmJ^{-1}$, respectively. Pyroelectric characteristics have been improved to twice the values for the $PbTiO_3$ ceramics containing small amounts of La and Mn. The spontaneous polarization Ps of the ceramics increases to a great extent in the Ca concentration range of x=0.20-0.30, and reaches larger values of 40-42 μ C/cm^2 than 33 μ C/cm^2 of the c-axis oriented sputtering $PbTiO_3$ thin film. With a decrease in the infrared ray absorbing film diameter, the responsivity Rv is improved to 140-180% in the range of 0.15-0.4Hz. The Responsivity Rv for the sensor with a Si filter window shows high values of 860 V/W.

It was found that the pyroelectric infrared sensor using $(Pb_{1-x}, Ca_x)[(Co_{1/2}W_{1/2})Ti]O_3$ ceramics is appropriate for use as a human body sensor.

Keywords : pyroelectric infrared sensor, infrared sensor, pyroelectricity, pyroelectric ceramics, modified lead titanate, ferroelectricity

1. Introduction

Recently, pyroelectric infrared sensors have been widely used in consumer electric appliances and other electric equipments, such as microwave ovens, automatic door systems, human body sensors and burglar alarm systems[1)-9)]. Pyroelectric infrared sensors show good sensing characteristics. Differing from photon sensors, they can be used at room temperature and their infrared response does not depend on the wavelength of the infrared rays used[3)]. The pyroelectric materials performance is represented by the figure of merit Fv, defined as $P/\varepsilon Cv$, where P, ε and Cv are pyroelectric coefficient, relative dielectric constant and volume specific heat, respectively. Nowadays, various kinds of pyroelectric materials, like $LiTaO_3$ single crystal, are commercially available and used. Among them, $(Pb, Ca)[(Co_{1/2}W_{1/2})Ti]O_3$ ceramics have been regarded as good pyroelectric materials, because of their large pyroelectric coefficient P, small dielectric constant ε, and high Curie temperature Tc[5),6)].

In this work, the pyroelectric properties and the infrared sensor characteristics for $(Pb, Ca)[(Co_{1/2}W_{1/2})Ti]O_3$ ceramics have been studied by changing Ca concentration, the infrared ray absorbing film diameter, and the electromagnetic wave shielding materials for packaging. These infrared sensors are assembled by hybrid IC technology.

2. Sample Preparation and Measurements

Figure 1 shows the pyroelectric ceramics manufacturing process. Raw materials, PbO, CoO, $CaCO_3$, WO_3, $MnCO_3$ and NiO, were calcined at 900 ℃ for 2 hours in air after weighing and mixing. The mixture were formed by die pressing and fired at 1100－1180 ℃ for several hours. Because of the low firing temperature and small amount of PbO vaporization, in comparison with PZT ($PbTiO_3$-$PbZrO_3$) ceramics, the mixture was not fired in PbO atmosphere. Both surfaces of the fired samples were polished until the samples were 0.5 mm thick and their diameter was 20 mm. After their polarization, they were polished again in the thickness of 100 μ m. Usually, $PbTiO_3$ ceramic polarization requires a markedly high voltage and high temperature, more than 60kV and 200℃, respectively[4)]. However, $(Pb, Ca)[(Co_{1/2}W_{1/2})Ti]O_3$ ceramics can be polled at lower voltage and temperature, 40-50kV/cm, 100℃, respectively, in silicone oil. Aging tests were performed for each sample.

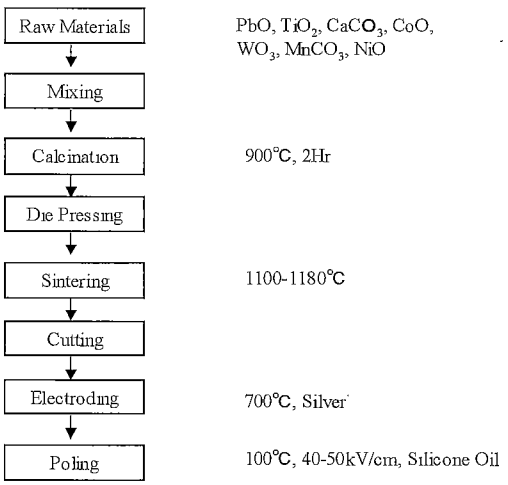

Fig. 1. Manufacturing process for $(Pb, Ca)[(Co_{1/2}W_{1/2})Ti]O_3$.

* Corporate R & D Center, Toshiba Corporation, 1, Komukai Toshiba –cho, Saiwai-ku Kawasaki 212-8582
** School of Science and Engineering, Waseda University, 3-4-1, Ohkubo, Shinjyuku-ku, Tokyo 169-8555
*** Toshiba Research Consulting Corporation, 1, Komukai Toshiba –cho, Saiwai-ku Kawasaki 212-8582

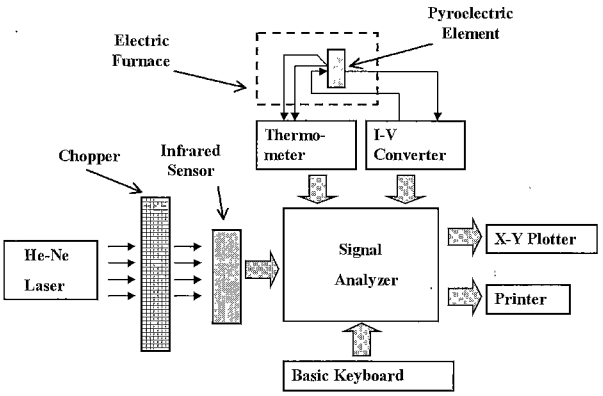

Fig. 2. Schematic diagram for measuring pyroelectric coefficient P, responsivity Rv and step irradiation pyroelectric voltage response.

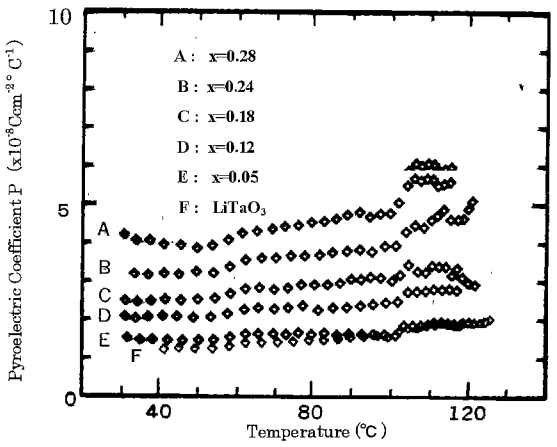

Fig. 3. Temperature dependence of pyroelectric coefficient P for (Pb1-x, Cax) [(Co1/2W1/2) Ti] 03.

Figure 2 shows the schematic diagram for measuring the pyroelectric coefficient P, the responsivity Rv and the step irradiation pyroelectric voltage response. The pyroelectric coefficient P can be expressed by the following equation.

$$P = (Ip/A)(dT/dt)^{-1} \quad \cdots\cdots (1)$$

where Ip, A, T, t are pyroelectric current, electrode area, temperature and time, respectively.

The spontaneous polarization Ps values were measured by the Sawyer-Tower method. The responsivity Rv, the specific detectivity, the step voltage response were measured under chopped light irradiation from He-Ne laser (Hughes Aircraft Co. Model 3221H-PC, Beam diameter: 3mm) by signal analyzer (Iwatsu Sm-2100A) and a spectrum analyzer (Hewlett Packard3582A). The relative dielectric constant ε values were measured by LCR meter(YHP-4261A) at 1 kHz.

3. Pyroelectric Properties of $PbTiO_3$ Ceramics

Figure 3 shows the temperature dependence of pyroelectric coefficient P for $(Pb_{1-x}, Ca_x)[(Co_{1/2}W_{1/2})Ti]O_3$ ceramics, comparing with that for $LiTaO_3$ single crystal having high Curie temperature of 618℃. In practical use, it is important that any

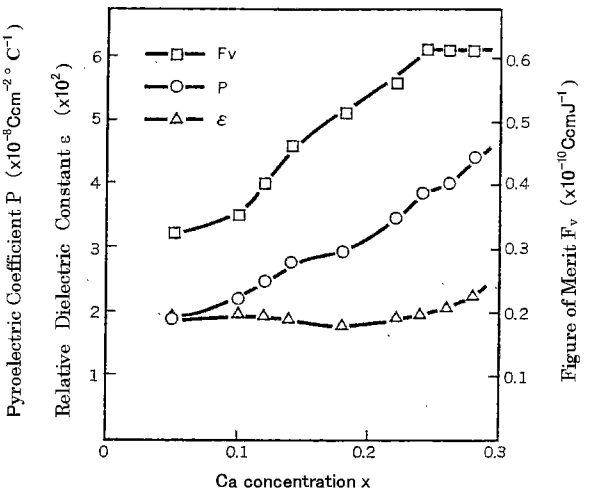

Fig. 4. Pyroelectric coefficient P, relative dielectric constant ε, and figure of merit Fv, for (Pb_{1-x}, Ca_x) $[(Co_{1/2}W_{1/2})Ti]$ O_3 as a function of Ca concentration.

variation in the pyroelectric coefficient P, caused by the ambient temperature increase, be as small as possible. In the case of Ca introduction into the host lattice from x = 0.05 to x = 0.28, the pyroelectric coefficient P value variations in the unit temperature are approximately 0-5x10^{-8}Ccm^{-2}℃$^{-1}$ and similar to that of 5x10^{-8}Ccm^{-2}℃$^{-1}$ for $LiTaO_3$ single crystal. These values are lower than that of approximately 7.5 x10^{-8}Ccm^{-2}℃$^{-1}$ for the representative $PbTiO_3$ ceramics containing small amount of La and Mn[11] and the C-axis oriented sputtering $PbTiO_3$ thin film[4]. In the case of from x = 0.05 to x = 0.28, the pyroelectric coefficient P for $(Pb_{1-x}, Ca_x)[(Co_{1/2}W_{1/2})Ti]O_3$ ceramics is hardly dependent on the temperature increase from room temperature to 100℃.

Figure 4 shows the pyroelectric coefficient P, the relative dielectric constant ε, and the figure of merit Fv, for $(Pb_{1-x}, Ca_x)[(Co_{1/2}W_{1/2})Ti]O_3$ as a function of Ca concentration. As Ca is introduced into $PbTiO_3$ ceramic, the pyroelectric coefficient increases to a great extent. In the Ca concentration of x = 0.28, the pyroelectric coefficient reaches 4.43 × 10^{-8} Ccm^{-2}℃$^{-1}$. The pyroelectric coefficient P for $PbTiO_3$ ceramic containing La and Mn, and the C-axis oriented sputtering $PbTiO_3$ thin film are 1.8 × 10^{-8}Ccm^{-2}℃$^{-1}$ and 3.0 × 10^{-8}Ccm^{-2}℃$^{-1}$, respectively[4][11]. The pyroelectric coefficient P for $(Pb_{1-x}, Ca_x)[(Co_{1/2}W_{1/2})Ti]O_3$ has been improved to 1.5-2 times those for the representative $PbTiO_3$ ceramics. Comparing with the pyroelectric coefficient P for the $LiTaO_3$ single crystal shown in Fig.3, that of 4.43 × 10^{-8} Ccm^{-2} ℃$^{-1}$ for $(Pb_{0.72}, Ca_{0.28})[(Co_{1/2}W_{1/2})Ti]O_3$ is 2-2.5 times larger than those of 1.8-2.2 × 10^{-8}Ccm^{-2}℃$^{-1}$ for $LiTaO_3$ single crystal. In addition, $(Pb_{1-x}, Ca_x)[(Co_{1/2}W_{1/2})Ti]O_3$ ceramics have many advantages such as low cost manufacturing and easy handling etc.

The change in the relative dielectric constant is markedly small. As Ca is introduced into the host lattice, the relative dielectric constant decrease slightly, until Ca concentration reaches x = 0.18. From x = 0.18 to x = 0.30, the dielectric constant increases gradually. Above x=0.30, it increases rapidly. Though another representative pyroelectric ceramic, PZT, has a

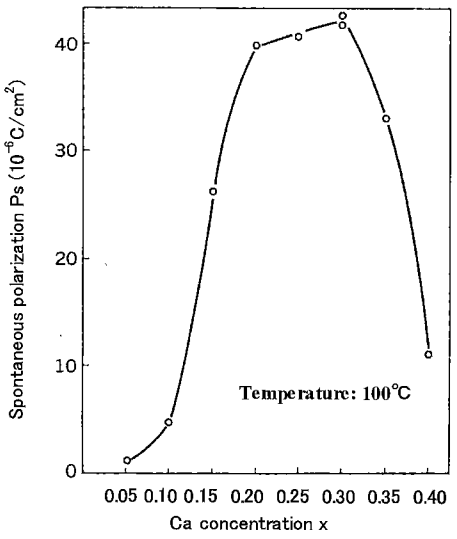

Fig. 5. Spontaneous polarization Ps for $(Pb_{1-x},Ca_x)[(Co_{1/2}W_{1/2})Ti]O_3$ ceramics.

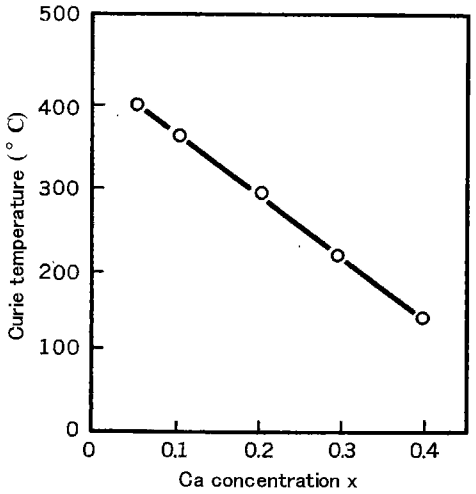

Fig. 6. Relation between Curie temperature and Ca concentration x of $(Pb_{1-x},Ca_x)[(Co_{1/2}W_{1/2})Ti]O_3$ ceramics.

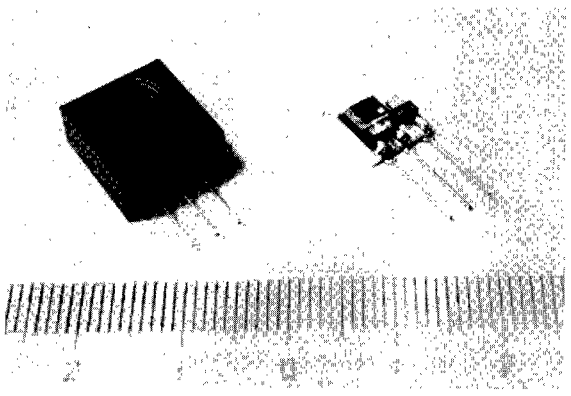

Fig. 7. Pyroelectric infrared sensor using $(Pb,Ca)[(Co_{1/2}W_{1/2})Ti]O_3$ ceramic and Hybrid IC Substrate.

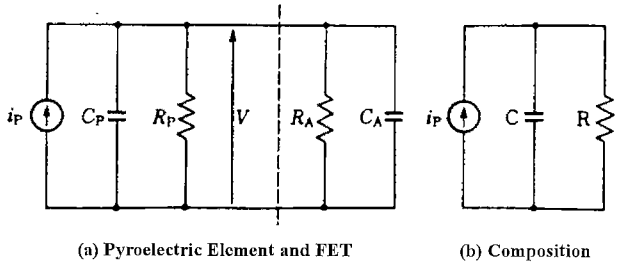

Fig. 8. Equivalent circuit of pyroelectric sensor.

large dielectric constant of 380-1800, (Pb, Ca)$[(Co_{1/2}W_{1/2})Ti]O_3$ ceramics have a low relative dielectric constant of approximately 200. The figure of merit Fv increases in the Ca concentration range from x = 0.05 to x = 0.24. From x = 0.24 to x = 0.28, the figure of merit Fv reaches a high value of 0.61 x 10^{-10}CcmJ^{-1}. At present, pure $PbTiO_3$ ceramic cannot be obtained, because of sintering difficulty. Therefore, compared with representative $PbTiO_3$ ceramic containing La and Mn, Fv has been improved to a great extent from 0.3 x 10^{-10}CcmJ^{-1} to 0.61 x 10^{-10} CcmJ^{-1}. It has been found that Ca introduction into $PbTiO_3$ ceramic exerts a great influence on the $PbTiO_3$ ceramic pyroelectric properties.

Figure 5 shows Ca concentration dependence of the spontaneous polarization Ps for $(Pb_{1-x},Ca_x)[(Co_{1/2}W_{1/2})Ti]O_3$ ceramics at 100℃. With an increase in the Ca concentration range of x = 0.05-0.20, the spontaneous polarization Ps increases to a great extent, and saturates in the Ca concentration range of x = 0.20-0.30. The spontaneous polarization Ps reaches high values of 40-42 μ C/cm^2 in the Ca concentration range of x = 0.20-0.30. These values are larger than 33 μ C/cm^2 of the C-axis oriented sputtering $PbTiO_3$ thin film[4], and a half of 75 μ C/cm^2 of the $PbTiO_3$ single crystal. In the Ca concentration range of more than x = 0.30, the spontaneous polarization decreases remarkably. In the lowest Ca concentration of x = 0.05, the spontaneous polarization Ps is as small as 1 μ C/cm^2. This value agrees well with 2-3.5 μ C/cm^2 of the representative $PbTiO_3$ ceramics containing small amount of La and Mn[11]. One of the main reason for the pyroelectricity improvement by the Ca introduction into $PbTiO_3$ host lattice is attributed to the increase in the spontaneous polarization Ps.

Figure 6 shows the relation between the Curie temperature and the Ca concentration x of $(Pb_{1-x},Ca_x)[(Co_{1/2}W_{1/2})Ti]O_3$ ceramics in order to clarify the reason of the pyroelectric coefficient increase. With an increase in Ca concentration x, the Curie temperature decreases from 400℃ at x = 0.05 to 300℃, 230℃ and 150℃ at x = 0.20, 0.28 and 0.40, respectively, according to the Vegard law. The Curie temperature of the single crystal $PbTiO_3$ and that of the $PbTiO_3$ ceramics containing small amount of La and Mn are 490℃ and 470℃, respectively. The value of the Curie temperature extrapolated to x = 0 in Fig. 6, is 440℃. This value agrees well with those values of the $PbTiO_3$ single crystal and ceramics. The spontaneous polarization Ps decrease in the high Ca concentration range of more than x = 0.30 as shown in Fig.5 is partly explained in terms of ferroelectricity decrease attributed to the Curie temperature decrease. Considering the soldering temperature in the sensor fabrication and the ambient temperature in practical use, it is to be desired that the Curie

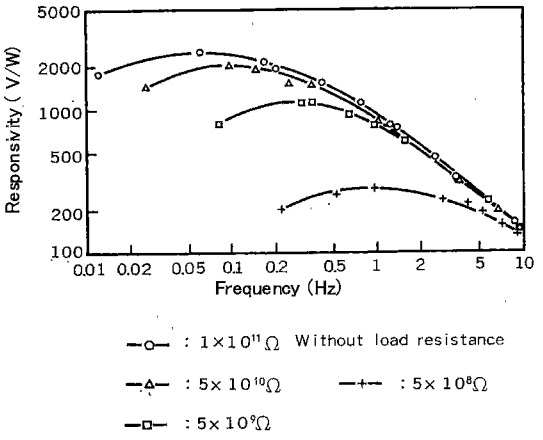

Fig. 9. Frequency dependence of responsivity Rv for the pyroelectric element with load resistance as a parameter.

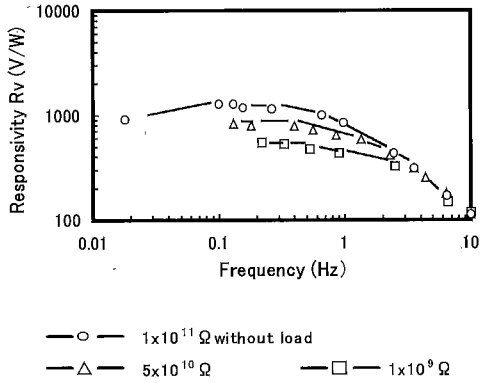

Fig. 10. Frequency dependence of responsivity Rv for sensor with a Si window with load resistance as a parameter.

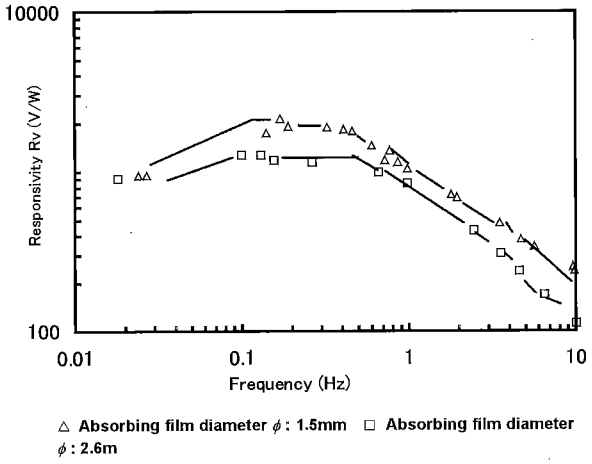

Fig. 11. Frequency dependence of responsivity Rv with infrared ray absorbing film diameter as a parameter.

temperature is higher than 200℃. $(Pb_{1-x}, Ca_x)[(Co_{1/2}W_{1/2})Ti]O_3$ ceramics(x = 0.05-0.30) qualify this requirement.

Thus, it is found that the main reason of the improvement in the pyroelectricity by the Ca introduction into $PbTiO_3$ host lattice is attributed to the increase in the spontaneous polarization Ps and the decrease in the Curie temperature.

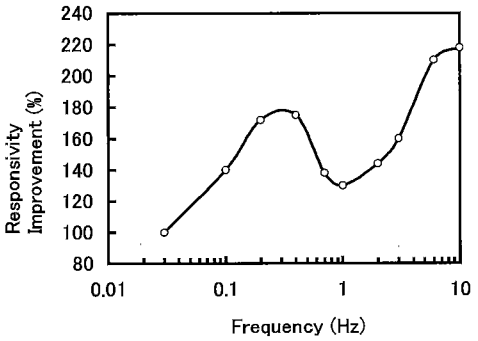

Fig. 12. Responsivity improvement by reducing infrared ray absorbing film diameter from 2.6mm to 1mm.

4. Sensor Structure

Figure 7 shows a pyroelectric infrared sensor using $(Pb_{0.76}, Ca_{0.24})[(Co_{1/2}W_{1/2})Ti]O_3$ ceramic and the hybrid IC substrate. The pyroelectric element has a 3 x 3 mm area and is 0.1 mm thick. Ni-Cr thin film in the thickness of 20nm is evaporated in order to absorb infrared rays on a surface of the pyroelectric element, because $PbTiO_3$ ceramics can absorb as little as 40% of infrared ray power[3]. Furthermore, the film is used as an electrode. The connecting electrode on the Ni-Cr thin film and the rear surface electrode are made of Ag paste in the thickness of 500nm. The pyroelectric element is mounted with other components, like an FET, on the substrate having a hole for thermal insulation by epoxy resign. The hole diameter is 3.0 mm. The low temperature fired ceramic substrate is used because of its markedly low thermal conductivity of approximately 3 W/mK. The sensor electric circuit consists of a set of interchangeable load resistance(10^8-10^{11} Ω),connected parallel to the pyroelectric element and a FET source follower circuit having 10kΩ resistance[1]. The equivalent circuit is shown in Fig.8. These infrared sensors are fabricated by hybrid IC technology.

5. Sensor Characteristics

5.1 Frequency Dependence of Responsivity Rv

Figures 9-10 show the chopping frequency dependence of responsivity Rv for the pyroelectric element and that for the sensor with a Si window with load resistance as a parameter, respectively. The infrared ray absorbing film diameter is 2.6 mm. The maximum responsivity of the peak shifts toward the frequency range lower than 1Hz, and further increases to a great extent. The resistance of the pyroelectric element has an appropriate value of 1 x 10^{11} Ω. Therefore, the sensor can operate without the load resistance. It is very useful for reduction in production cost, and wiring simplification. Human body sensing requires a high responsivity value in the less than 1Hz low frequency range. This sensor is remarkably applicable for use as a human body sensor. The pyroelectric infrared response does not depend on the wavelength of the infrared rays used. However, the performance is affected by window materials. The pyroelectric element and the sensor with Si filter window show high responsivity Rv values of 2480 V/W and 1440 V/W at 0. 1 Hz, respectively.

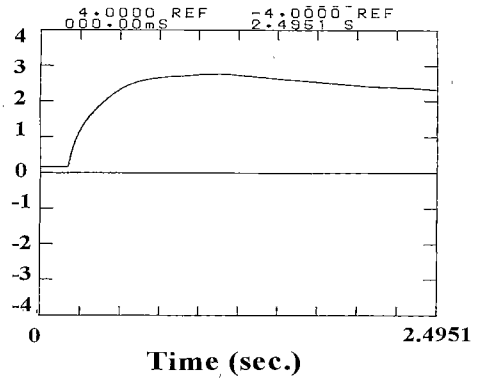

(a) Rise

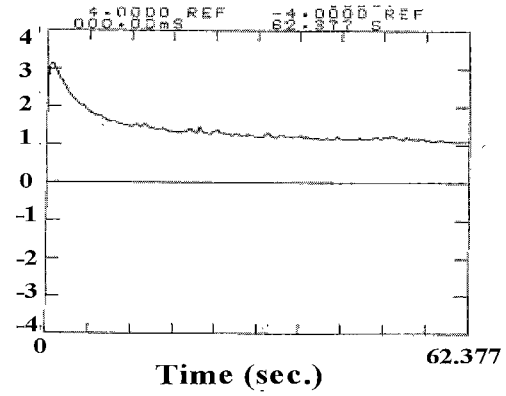

(b) Fall

Fig. 13. Sensor response of infrared sensor with infraed ray absorbing film diameter'1.5mm.

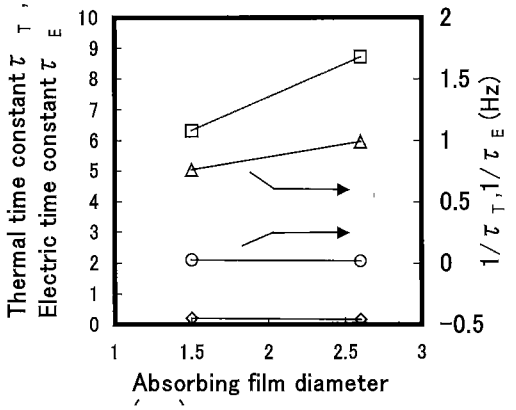

Fig. 14. Change in thermal time constant τ_T and electric time constant τ_E with decreasing infrared ray absorbing film diameter.

5.2 Effects of Infrared Ray Absorbing Film Diameter

5.2.1. Responsivity Rv Figure 11 shows the chopping frequency dependence of responsivity Rv for the sensor with a Si window with infrared ray absorbing film diameter as a parameter. There is a tendency as well as in Fig.10 that the maximum responsivity in the both sensors is located in the frequency range of lower than 1Hz. Moreover, with a decrease

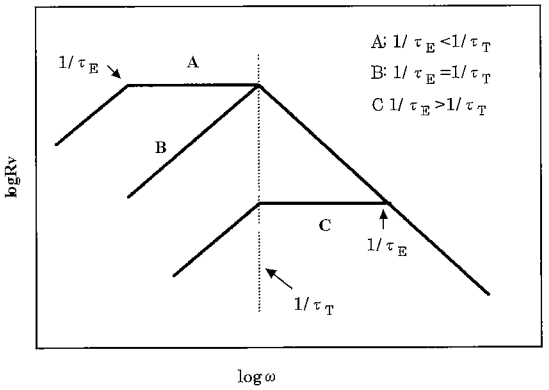

Fig. 15. Schematic diagram of angular frequency dependence of responsivity Rv.

of the infrared ray absorbing film diameter from 2.6 mm to 1.5 mm, the responsivity Rv increases in the frequency range of 0.03-10Hz. The improvement of the responsivity Rv is indicated in Fig.12. The responsivity Rv has been improved to180% in the range of 0.15-0.4Hz, 130-180% in the range of 0.1-1Hz, and 220% at 10Hz. The responsivity Rv for the sensor with a Si window reaches 2000V/W in the range of 0.15-0.4Hz. The reduction of the absorbing film area is useful for improving the responsivity.

5.2.2. Electric and Thermal Time Constant Since the electric time constant τ_E and the thermal time constant τ_T exert a great influence on the responsivity Rv, they have been investigated to clarify the increase of Rv with decreasing the infrared ray absorbing film area. The equivalent circuit of the pyroelectric infrared sensor is shown in Fig. 8. The rise in temperature changes the spontaneous polarization Ps of the pyroelectric element, causing a charge flow through it and the load in the circuit. For step irradiation, the pyroelectric voltage response V(t) is represented by the next equation[1),(12)].

$$V(t)= \xi F_0 (1/\tau_E - 1/\tau_T)^{-1} \{\exp(-t/\tau_T) - \exp(-t/\tau_E)\} \quad \cdots\cdots (2)$$

Here τ_E = RC(R: Composite resistance, C: Composite capacitance), τ_T =H/G (H: Thermal capacitance, G: Thermal conductance), F_0 is the initial radiation power absorbed per unit area of the pyroelectric element, ξ is a material constant of PA^2/CH. Because $\xi F_0 (1/\tau_E - 1/\tau_T)^{-1}$ is constant for a given condition, the pyroelectric voltage response is proportional to $\{\exp(-t/\tau_T) - \exp(-t/\tau_E)\}$. The response V(t) is symmetrical with respect to τ_T and τ_E. In the case that τ_T and τ_E differ appreciably, the rise of the response depends on the smaller time constant and the fall of the response depends on the larger one between τ_T and τ_E. The calculated values of τ_E are approximately 9 seconds from the composite resistance R and the composite capacitance. For $\tau_T \ll \tau_E$, the rise and fall step response are represented by the next equations, respectively.

$$V(t)= \xi F_0 \tau_T \{1-\exp(-t/\tau_T)\}$$
$$=Vp \{1-\exp(-t/\tau_T)\} \quad \cdots\cdots (3)$$

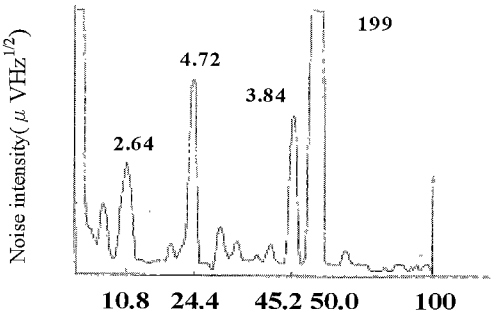

(a) Pyroelectric element

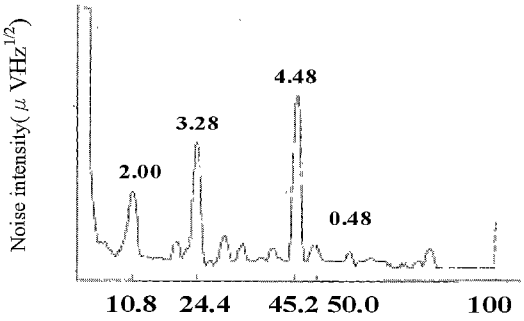

(b) Sensor with Al metal package

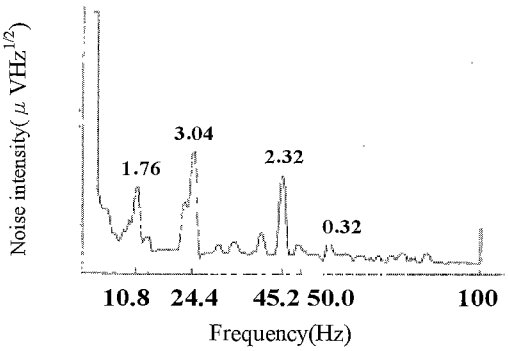

(c) Sensor with Ni conductive paint coated ABS resign package

Fig. 16. Frequency dependence of noise intensity in.

$$V(t)= \xi F_0 \tau_T \exp(-t/\tau_E) = Vp \exp(-t/\tau_E) \quad \cdots\cdots (4)$$

Here Vp is the peak value of the voltage response.
Therefore, the thermal time constant τ_T and the electric time constant τ_E have been measured as the time at the pyroelectric voltages of 63.2% and 36.8% values for the peak voltages in the rising and falling relaxation phenomenon, respectively.

Figures 13(a) -13(b) show the rise and fall step response curves for infrared ray power switching in the sensor with the infrared ray absorbing film diameter of 1.5mm, corresponding to the thermal time constant τ_T and the electric time constant

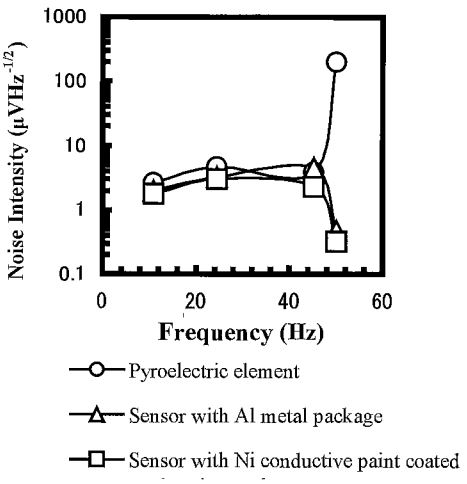

Fig. 17. Peak noise intensity at four frequencies of 10.8Hz, 24.4Hz, 45.2Hz, and 50.0Hz.

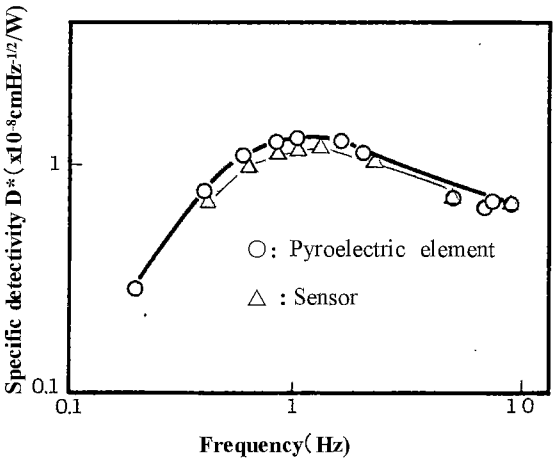

Fig. 18. Specific detectivity D* of pyroelectric element and sensor with Si filter window.

τ_E. The curves indicate no big noise and have good repeatability. Figure 14 shows the change in the thermal time constant τ_T and the electric time constant τ_E with decreasing the infrared ray absorbing film diameter. The frequency of $1/\tau_T$ and $1/\tau_E$ are also indicated in Fig.14. The thermal time constant τ_T increases from 0.161 seconds to 0.208 seconds with decreasing the infrared ray absorbing film diameter from 2.6mm to 1.5mm. The reason may be explained by that it takes longer time for the heat to be propagated to the edges of pyroelectric element having the infrared ray absorbing film diameter of 1.5mm, comparing with the heat propagation time for the element having that of 2.6mm, because the size of the pyroelectric element, 3 x 3 x 0.1mm, and fabrication method are the same in both the elements. On the contrary, the electric time constant τ_E reduces from 8.73 seconds to 6.32 seconds with decreasing the infrared ray absorbing film diameter. The reason is not clear, because the capacitance C is decreased and the resistance R is increased with decreasing the infrared ray absorbing film area so that the electric time constant τ_E = RC should not be changed and kept constant value.

The frequency of $1/\tau_T$ is decreased from 0.99Hz to 0.76Hz and $1/\tau_E$ is increased from 0.0182Hz to 0.0252Hz with

decreasing the absorbing film diameter. there is still the relationship of $1/\tau_E < 1/\tau_T$ as shown in Fig.14.

5.2.3. Theoretical Analysis The responsivity Rv is the ratio of the sensor output voltage V to the incident infrared ray energy I, and represented by the next equation.

$$Rv = V/I = V/SW = \eta\,\omega PARG^{-1}(1+\omega^2\tau_E^2)^{-1/2}(1+\omega^2\tau_T^2)^{-1/2} \quad \cdots\cdots (5)$$

η : Emissivity , ω : Angular frequency,
P: Pyroelectric coefficient, S: Irradiation area,
R: Composite resistance G: Thermal conductance,
τ_E: Electric time constant, τ_T: Thermal time constant

The angular frequency, $\omega = 2\pi f$(f: frequency), the electric time constant τ_E, and the thermal time constant τ_T, exert a great influence on the responsivity. The responsivity Rv depends on the angular frequency ω, and is changed by the value of $1/\tau_T$ and $1/\tau_E$. Figure 15 shows the schematic diagram of the angular frequency dependence of responsivity Rv. In Fig.15, $1/\tau_T$ keeps the constant value and $1/\tau_E$ changes with increasing the angular frequency. Three different dependencies of A, B and C are obtained, corresponding to the relation of $1/\tau_E < 1/\tau_T$, $1/\tau_E = 1/\tau_T$, and $1/\tau_E > 1/\tau_T$. For getting high responsivity, especially, in the low frequency of less than 1Hz for human detecting, the angular frequency dependence of A is used. The frequency dependence of the responsivity Rv in Fig. 11 is in good agreement with the above theoretical dependence of A. The responsivity Rv increased to a great extent in the frequency region of 0.02-0.7Hz. The frequencies corresponding to $1/\tau_T$ and $1/\tau_E$ of the pyroelectric infrared sensor are located around in the frequency range of 0.76-0.99Hz and 0.018-0.025Hz, respectively as shown in Fig. 14. Though the infrared ray absorbing film area is decreased, there is still the relationship of $1/\tau_E < 1/\tau_T$. Those values of $1/\tau_T$ and $1/\tau_E$ are almost coincide with the both end of the responsivity saturation region in the trapezoidal dependency curves in Fig. 11.

The increase of Rv with decrease in the infrared ray absorbing film diameter can be partly explained by the below discussion.

In the case that the dependency of A at the relation of $1/\tau_E < 1/\tau_T$ is still sustained, the following three equation (6), (7), and (8) are derived from the equation (5) in the dependency of A, corresponding to the relation $\omega > 1/\tau_T$, $1/\tau_E < \omega < 1/\tau_T$, and $\omega < 1/\tau_E$, respectively[5].

$$Rv = \eta P(Cv\,\varepsilon\,\varepsilon_0)^{-1} S^{-1}\omega^{-1} \quad \cdots\cdots (6)$$
$$Rv = \eta P(Cv\,\varepsilon\,\varepsilon_0)^{-1} S^{-1}\tau_T \quad \cdots\cdots (7)$$
$$Rv = \eta PR(Cvt)^{-1}\tau_T\,\omega \quad \cdots\cdots (8)$$

At the relation of $1/\tau_E < \omega < 1/\tau_T$, the responsivity Rv is directly proportional to the thermal time constant τ_T. The average Rv improvement values of 150% at the relation of $1/\tau_E < \omega < 1/\tau_T$ in the frequency range of 0.03-0.7Hz in Fig. 11 and Fig. 12, are almost in good agreement with the thermal constant increase from 0.161seconds (100%) to 0.208seconds(129%) in Fig.14. The responsivity Rv increase with decrease in the infrared ray absorbing film diameter might be attributed to the τ_T increase from the equation (8). The responsivity Rv also increases around at 10Hz in the region of $\omega > 1/\tau_T$. The reason is not clear at present.

It was found that responsivity Rv increases with a decrease in the infrared ray absorbing film diameter on $(Pb_{1-x}, Ca_x)[(Co_{1/2}W_{1/2})Ti]O_3$ ceramics as long as at the relationship of $1/\tau_E < 1/\tau_T$ is sustained.

5.3. Electro-magnetic Interference The electro-magnetic interference gives a great influence on the sensor characteristics, because of low electric signals caused by pyroelectricity[13]. Figure 16 shows the frequency dependence of the noise intensity In of the pyroelectric element, the sensor with Al metal package, and the sensor with Ni conductive paint coated ABS resign package, in the frequency range of less than 100Hz, respectively. In order to choose the low noise intensity package, the noise intensity measurement was carried out and the measured values were accumulated in 16 times repeatedly. The resistivity and the thickness of the Ni conductive paint are 2.5×10^{-3} Ωcm and 50 μm. There is a lot of research on the electro-magnetic interference in the frequency range from 10KHz to 1GHz, especially from 1MHz to 1GHz. However, the research in the low frequency range of 0-100Hz are markedly few[13]. In Fig.16, there are four large noise peaks located at 50Ha, 45.2Hz, 24.4 Hz and 10.8Hz for the pyroelectric element and the sensors. Figure 17 shows the peak noise intensity at the above-mentioned four frequencies. The noise intensities for the sensors with Ni conductive paint coated ABS resign package and with Al metal package are lower than those of the pyroelectric element in every frequency range, especially, markedly lower at 50Hz. Moreover, there is a tendency that the noise intensities for the sensor with Ni conductive paint coated ABS resign package is lower than those for the sensor with Al metal package. Ni conductive paint coated ABS resign package is very effective in the electro-magnetic interference for the pyroelectric infrared sensor.

5.4. Specific Detectivity D* Figure 18 shows the specific detectivity D* of the pyroelectric element, and the sensor with a Si filter window. Though the pyroelectric infrared response does not depend on the wavelength of the infrared rays used, the specific detectivity D* as well as the responsivity Rv is affected by window materials. The pyroelectric element and the sensor with a Si filter window show high specific detectivity D* values of 1.3 $\times10^8$ $cmHz^{-1/2}/W$ and 0.81 $\times10^8$ $cmHz^{-1/2}/W$ at 1 Hz, respectively.

6. Conclusion

Pyroelectric properties and infrared sensor characteristics for $(Pb_{1-x}, Ca_x)[(Co_{1/2}W_{1/2})Ti]O_3$ ceramics have been studied by changing Ca concentration, the infrared ray absorbing film diameter, and the electromagnetic wave shielding materials for packaging. With an increase in Ca concentration from x = 0.05 to 0.28, the pyroelectric coefficient P and the figure of merit Fv increased and reached 4.43 x 10^{-8} $Ccm^{-2}℃^{-1}$, and 0.61 x 10^{-10} $CcmJ^{-1}$, respectively. Pyroelectric characteristics have been improved to twice the values for the $PbTiO_3$ ceramics containing small amounts of La and Mn. As the Ca concentration increases, the spontaneous polarization Ps of the ceramics increases to a great extent in the Ca concentration range of x = 0.20-0.30, and reaches larger values of 40-42 μ C/cm^2 than 33 μ C/cm^2 of the c-axis oriented sputtering $PbTiO_3$ thin film. The Curie temperature decreases according to the

Vegard law. The results indicate that the improvement in the pyroelectricity by the Ca introduction into $PbTiO_3$ host lattice is attributed to the increase in the spontaneous polarization Ps and the decrease in the Curie temperature.

The sensor can operate without the load resistance. The maximum responsivity Rv value versus chopping frequency is obtained in a less than 1Hz frequency range. Moreover, with a decrease in the infrared ray absorbing film diameter from 2.6 mm to 1.5 mm, the responsivity Rv for the sensor with a Si window is improved to 140-180% and reaches 2000V/W in the range of 0.15-0.4Hz. The responsivity Rv increase with decrease in the infrared ray absorbing film diameter can be theoretically explained in terms of the τ_T increase and the sustaining relationship of $1/\tau_E < 1/\tau_T$. The reduction of the absorbing film area is useful for improving the responsivity. The noise intensities for the sensor with Ni conductive paint coated ABS resign package is lower than those for the sensor with Al metal package. Ni conductive paint coated ABS resign package is very effective in the low noise frequency range. The Responsivity Rv and the relative detectivity D* for pyroelectric element and the sensor with a Si filter window show high values of 1000 V/W, 1.3 $x10^8$ $cmHz^{-1/2}/W$, and 860 V/W, 0.81 x $10^8 cmHz^{-1/2}/W$, at 1 Hz, respectively.

It has been found that the pyroelectric infrared sensor using $(Pb_{1-x}, Ca_x)[(Co_{1/2}W_{1/2})Ti]O_3$ ceramic is appropriate for use as a human body sensor.

(Manuscript received Nov. 6, 2001, revised Apr. 23, 2002)

References

(1) T Ishigaki, K Nakamura, and E Yamaka . "Pyroelectric infrared detector within a TO-5 package", *National Tech. Rept.*, **24**, 453 (1978)

(2) K Shigiyama : "PVDF pyroelectric infrared detector", *National Tech. Rept.*, **26**, p 517 (1980)

(3) E. Yamaka, T. Hayashi, M Matsumoto K Nakamura, K. Shigiyama, M. Akiyama, and K. Kitahori : "Pyroelectric infrared detector", *National Tech. Rept.*, **18**, 141 (1972)

(4) K. Iijima, S. Kawashima, and I. Ueda . "Pyroelectric infrared detector made of c-axis oriented $PbTiO_3$ thin film", Proc. 3rd Sensor Symp , 133 (1983)

(5) M. Nakamoto, Y. Hirao, Y. Yamashita, and N. Iwase : "Pyroelectric infrared sensor using (Pb, Ca) $[(Co_{1/2}W_{1/2})Ti]$ O_3 ceramics", Proc 4th Sensor Symp., 209 (1984)

(6) Y. Iida and Toyoda "Fundamental Characteristics of pyroelectric infrared detectors having surface electrode", *T. IEE Japan*, **93** (1977)

(7) M. Okuyama, H. Seto, M Kojima, Y Matsui, and Y. Hamakawa : "Integrated pyroelectric infrared sensor using PbTiO3 thin film", *Jpn. J. Appl. Phys.*, **22** Suppl. 22-1, 465(1983)

(8) M. Okuyama, Y. Togami, Y. Hamakawa , M. Kimata, and M Denda : "Room-temperature-oriented infrared image CCD sensor using pyroelectric gate coupled by dielectric signals of infrared radiation in Triglycine Sulphate and Strontium-Barium Niobate", *J. Appl. Physics*, **42**, 3741 (1971)

(9) M. Okuyama, T. Imai, and Y. Hamakawa : "Preparation of PbTiO3 thin films by Laser abration", *Integrated Ferroelectrics*, **1**, 333 (1992)

(10) T. D. Thanh, and N. Iwase : "Low temperature fired ceramic substrate", *IECE Trans.*, **CPM83-38**, 17 (1983)

(11) S Ikegami, Ichiro Ueda, and Takashi Nagata : "Electromechanical Properties of $PbTiO_3$ ceramics containingLa and Mn", *J. Acoust. Soc. Am.*, **50**, 1060 (1971)

(12) M. Simhoney, and A Shaulov : "Pyroelectric voltage rsponse to step signals of infrared radiation in Triglycine Sulphate and Strontium-Barium Niobate", *J. Appl. Phys.*, **42**, 3741 (1971)

(13) K. Nakayama and M. Kera : "EMI regulations and their future", *Kougyou Zairyou*, **10**, 26 (1984)

Masayuki Nakamoto (Member) was born in Tokyo, Japan, in 1951. He received the B. S. and M. S. degree in electronic material chemistry from Yokohama National University in 1975 and 1977, respectively. Since joining Toshiba corporation in 1977, he has been doing research on the rare-earth phosphors, the pyroelectric infrared sensors, which are commercialized and now widely used for high efficient tricolor fluorescent lamps and human body detecting sensors respectively, and the magneto-optical sensors using ferromagnetic materials. His current research interest is focused on vacuum microelectronics and NEMS. He was a Visiting Scientist of Massachusetts Institute of Technology (1986-1988) and a Symposium Chairman of the Electrochemical Society(1983-1988). He is a member of Japan Society of Applied Physics, and Phosphor Society of Japan.

Noboru Ichinose (Member) was born in Japan in 1935. He received the B. S. and Doctor degree from Waseda University. He joined Toshiba Corporation in 1959 and has been a professor of Waseda University from 1985. His current interests are functional ceramics and sensors including pyroelectric infrared sensors. He is a member of Japanese Ceramic Society and IEEE CPMT.

Nobuo Iwase (Non-member) was born in Japan in 1944. He received MEE degree from Chuo University in 1970 and Dr. Eng. degree from Hosei University in 1996. He joined Toshiba Corporation in 1970, where he engaged in development of microwave passive and active devices, and ceramic substrates and packages. Dr. Iwase is a member of IEEE CPMT and Institute of Electronics, Information and Communication Engineers (IEICE).

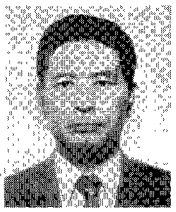

Yohachi Yamashita (Non-member) was born in Kagoshima prefecture Japan in 1951. He joined Toshiba Corp. Research and Development Center in 1969. He obtained his Doctor Degree in Materials Science from Waseda University in 1998. His research activities are Piezoelectric Materials and relaxors-lead titanate single crystals for medical transducers. He is an author and co-author of more than 90 scientific papers and 12 filed foreign patents. He was rewarded the Richard M. Fulrath Pacific Awards from the American Ceramic Society in 1993.He is a member of American Ceramic Society, Japanese Ceramic Society, and Japan Society of Applied Physics.